SC-R-66-1002

January 1967

Reprint

SHOCK-WAVE COMPRESSION OF 30% Ni-70% Fe ALLOYS: THE PRESSURE-INDUCED MAGNETIC TRANSITION

R. A. Graham

David H. Anderson

J. R. Holland

SANDIA CORPORATION

PRIME CONTRACTOR TO THE U.S. ATOMIC ENERGY COMMISSION

ALBUQUERQUE, NEW MEXICO; LIVERMORE, CALIFORNIA; TONOPAH, NEVADA

Issued by Sandia Corporation,
a prime contractor to the
United States Atomic Energy Commission

Reprinted from JOURNAL OF APPLIED PHYSICS, Vol. 38, No. 1, 223–229, January 1967
Printed in U. S. A.

Shock-Wave Compression of 30% Ni–70% Fe Alloys: The Pressure-Induced Magnetic Transition*

R. A. GRAHAM, DAVID H. ANDERSON, AND J. R. HOLLAND
Sandia Laboratory, Albuquerque, New Mexico
(Received 11 April 1966; in final form 29 July 1966)

The compressibility of 30% Ni–70% Fe (wt %) in the fcc phase is investigated from atmospheric pressure to 40 kbar with shock-wave loading techniques. The experiments are accomplished utilizing projectile impact techniques with stress profile measurements by the quartz gauge. A sharp change in compressibility indicates a second-order ferromagnetic Curie point transition at a stress of 25 kbar and a volume of 0.9807 V_0. The coefficient of Curie temperature change with pressure is found to be -5.8 ± 0.3°C kbar^{-1}. The agreement of this value with previous magnetic measurements, along with the anomalously large compressibility below the transition and the large decrease in compressibility at an elevated temperature, clearly indicates that this transition is a ferromagnetic to paramagnetic transition. Values for the change of thermal expansion and specific heat at the transition are computed from the Ehrenfest relations. These values are consistent with the magnetic character of the transition and give a complete description of the thermodynamic properties of the transition. To provide more compressibility data on various types of ferromagnetic materials, a few additional measurements are reported for Invar and 30% Ni–70% Fe in the bcc phase.

INTRODUCTION

UNUSUAL physical properties which are strongly correlated with unusual magnetic properties are characteristic of the alloys of about 30% to 40% Ni in Fe.[1] It is known that the Curie temperature and saturation magnetization of these alloys show an enormous sensitivity to pressure, reflecting a strong volumetric dependence of the magnetic interactions.[2,3] This strong pressure dependence of the magnetic order has allowed a number of investigations of the volumetric dependence of the magnetic order with the use of relatively low (5 kbar) pressures.[4] From these previous investigations it appears, as we will show, that the change in compressibility associated with the change in magnetic interactions is large enough to be readily measured in shock-wave compression experiments. Thus, a study of the thermodynamic properties of the pressure-induced magnetic transition appears promising. It is the object of this paper to report an investigation of the shock-wave compression of 30% Ni–70% Fe in the fcc phase which has resulted in the identification and determination of the thermodynamic properties of the pressure-induced ferromagnetic to paramagnetic transition. There appears to be no previous identification of a pressure-induced second-order phase transition under shock-wave compression.

BACKGROUND AND THEORY

The transition from a ferromagnetic to a paramagnetic state is normally considered to be a classic second-order phase transition; that is, there are no discontinuous changes in volume V or entropy S, but there are discontinuous changes in the volumetric thermal expansion β, compressibility k, and specific heat C_p. The relation among the variables changing at the transition is given by the Ehrenfest relations,

$$\Delta k_T = \Delta\beta(d\theta/dP), \tag{1}$$

and

$$\Delta C_p = TV\Delta\beta(d\theta/dP)^{-1}; \tag{2}$$

where Δ indicates the change occurring at the transition, k_T is the isothermal compressibility $-V^{-1}(dV/dP)_T$, and $d\theta/dP$ is the coefficient of Curie temperature change with pressure. It is clear from Eqs. (1) and (2) that a measurement of Δk_T and $d\theta/dP$ will result in a complete description of the thermodynamic properties of the transition.

The alloys of from 30% to 40% Ni in iron are noted for their unusual volumetric behavior. For example, it is well known that the thermal expansion of these alloys is anomalously low, with the Invar composition (36% Ni) having a thermal expansion close to zero at room temperature. Further, the atmospheric pressure compressibilities are anomalously large while the atomic lattice spacing and density data show strong departures from Vegard's law in this same composition range.[5,6]

For alloys containing up to about 27% Ni in Fe, the equilibrium phase at room temperature is bcc. However, in the neighborhood of 30% Ni either the fcc or bcc phases can be obtained at room temperature as the result of various heat treatments.[7] For nickel concentrations greater than 30%, the structure is fcc. Hence, the unusually large volumetric phenomena are characteristic of the fcc phase.

* This work was supported by the United States Atomic Energy Commission.

[1] Compositions are given in wt % unless otherwise specified.

[2] L. Patrick, Phys. Rev. **93**, 384 (1954).

[3] J. S. Kouvel and R. H. Wilson, J. Appl. Phys. **32**, 435 (1961).

[4] J. S. Kouvel, in *Solids Under Pressure*, W. Paul and D. M. Warschauer, Eds. (McGraw-Hill Book Company, Inc., New York, 1963).

[5] E. A. Owen, E. L. Yates, and A. H. Sully, Proc. Phys. Soc. (London) **49**, 315 (1937).

[6] A summary of physical and mechanical property data for Invar is given in: W. S. McCain and R. E. Maringer, "Mechanical and Physical Properties of Invar and Invar-Type Alloys," DMIC Memorandum 207 (August, 1965), Defense Metals Information Center, Battelle Memorial Institute.

[7] M. Hansen, *Constitution of Binary Alloys* (McGraw-Hill Book Company, Inc., New York, 1958), p. 677–684.

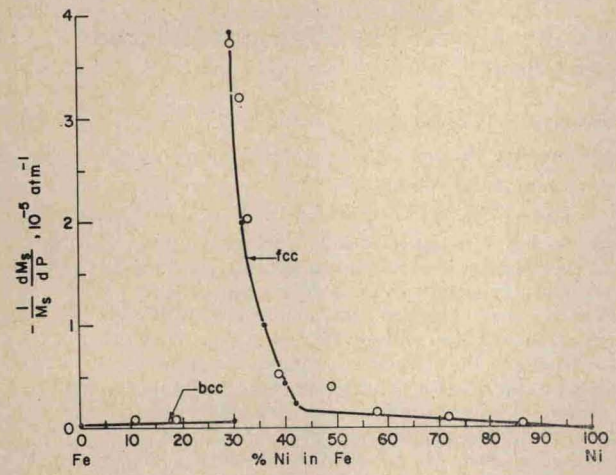

FIG. 1. Pressure dependence of the saturation magnetization of the Fe–Ni alloy system. The filled circles are data from Ref. 3 and the open circles are data from Ref. 8. Compositions are in atomic percent.

The pressure sensitivity of the magnetic properties of the Invar type alloys is indicated by extensive measurements[3] of the coefficient of saturation magnetization change with pressure $M_s^{-1}dM_s/dP$ for various compositions as shown in Fig. 1.[8] The exceedingly large values in the 30%–40% Ni range are evident and much in excess of the values for iron and nickel. The 30% Ni composition in the fcc phase is the most sensitive to pressure while this composition in the bcc phase is insensitive to pressure although strongly ferromagnetic.[3]

The change in compressibility expected if the transition occurs can be estimated from Eq. (1), since values for $d\theta/dP$ have been measured at low pressure and a value can be estimated for $\Delta\beta$. The value for $d\theta/dP$ measured by Patrick[2] for fcc 30%Ni–70%Fe is -5.7°C kbar^{-1} while the value for the bcc phase is about -0.3°C kbar^{-1}. The Curie temperature for the fcc alloy is 155°C while that for the bcc alloy is about 700°C.[4] On the basis of these values the expected behavior if the transition occurs is a large, easily detected change in compressibility at a pressure of 23 kbar for the fcc alloy and an anomalously large compressibility below the transition. On the other hand, the compressibility of the bcc alloy should exhibit normal behavior in this pressure range.[9] Hence, a measurement of the compressibility of fcc and bcc 30% Ni–70% Fe alloys to pressures of about 40 kbar should result in definite conclusions concerning the transition and the effect of magnetic interactions on shock-wave compressibility. Selection of the alloy 30% Ni–70% Fe for this investigation was based upon this unique combination of properties in the two phases and the exceptionally large coefficient of Curie temperature change with pressure for the fcc phase.

Plane shock-wave loading experiments yield precise stress–volume measurements; hence, they are a convenient method for observing the expected transition. A recently developed gun with essentially continuous control on the stress imparted to a sample[10] (~2 kbar increments) coupled with the excellent time resolution available with the quartz gage[11] provide a sound basis for measurements in this pressure range.

Curran[12] has pointed out that under certain unusual conditions the second-order phase transition might cause a cusp in the stress–volume relation resulting in a multiple wave structure as is the case for a first-order transition. His shock-wave compression measurements on Invar (36%Ni–64%Fe) showed large compressibilities in the low stress region but no distinct transition. In order to verify his results, we have also performed a few experiments on Invar.

EXPERIMENTAL PROCEDURE

Shock-wave loading is accomplished by the planar impact in vacuum of two flat disks. The stationary specimen disk is mounted on the muzzle of a compressed gas gun and the other disk is attached to the impact face of a projectile which is accelerated to various velocities by the gun. Shock-wave velocity measurements and measurements of the shock-wave stress–time profile with the quartz gage at a plane some distance from the impact surface are sufficient to compute the stress–volume relation for the shocked sample from the conservation of mass and momentum relations.[13] Precision is maintained in all alignment tolerances such that the "tilt" of one surface relative to the other at impact is typically 5×10^{-4} rad. A schematic of this method of performing the shock-wave experiment is shown in Fig. 2.

The gun experiment permits an additional measurement to those possible when high-explosive loading is

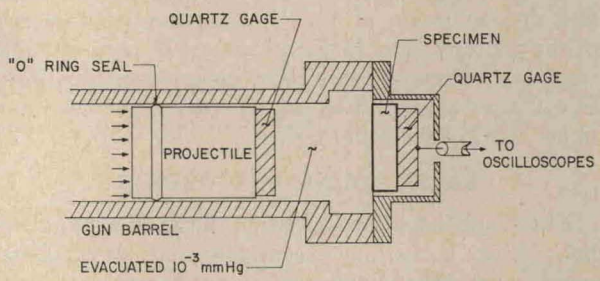

FIG. 2. Schematic diagram of the shock-wave experimental arrangement. In some of the experiments, the quartz gauge on the projectile is replaced by a facing of the specimen material.

[8] H. Ebert and A. Kussman, Physik. Z. **38,** 437 (1937).

[9] A first-order transition is known to occur in the bcc alloy at a stress of 83 kbar. R. G. McQueen, in *Metallurgy at High Pressures and High Temperatures* (Gordon and Breach Science Publishers, Inc., New York, 1964).

[10] S. Thunborg, G. E. Ingram, and R. A. Graham, Rev. Sci. Instr. **35,** 11 (1964).

[11] R. A. Graham, F. W. Neilson, and W. B. Benedick, J. Appl. Phys. **36,** 1775 (1965).

[12] D. R. Curran, J. Appl. Phys. **32,** 1811 (1961).

[13] G. E. Duvall, in *Response of Metals to High Velocity Deformation* (Interscience Publishers, Inc., New York, 1961).

TABLE I. Summary of shock-wave compression measurements on 30% and 36% Ni–Fe alloys.

u_0[a] (mm/μsec)	Specimen thickness (mm)	Impact Surface u_i[b] (mm/μsec)	Impact Surface σ_i[c] (kbar)	Propagated Profile U_{se}[d] (mm/μsec)	Propagated Profile σ_e[f] (kbar)	Propagated Profile $(V/V_0)_e$[g]	Propagated Profile σ_p[h] (kbar)	Propagated Profile $(V/V_0)_p$[i]	Propagated Profile u_p[j] (mm/μsec)
30% Ni–70% Fe fcc									
0.2709	12.81	0.1355	...	5.06	4.6	0.9978	45.4	0.9688	0.1313
0.3737	9.538	...	38.5	5.05	4.2	0.9980	40.2	0.9719	0.1167
0.3247	9.538	...	34.4	5.14	4.1	0.9980	34.4	0.9752	0.1018
0.2921	9.525	...	30.0	4.99	3.9	0.9981	29.0	0.9784	0.0872
0.2483	9.525	...	25.8	4.97	2.9	0.9986	25.0	0.9806	0.0749
0.2324	9.525	...	24.0	4.98	3.9	0.9982	23.5	0.9823	0.0702
0.1234	12.81	0.0617	...	5.02–5.00	4.7	0.9977	20.7[k]	0.9847	...
0.0902	12.81	0.0451	...	...	4.4	0.9980	15.9	0.9884	0.0465
0.1380	...	0.0396[l]	14.9[l]	...	...	...	...	0.9914[l]	...
Mean density 8.158 g/cm³; C_0=5.01 mm/μsec[m]; C_s=2.92 mm/μsec[n]; $\bar{\sigma}_e$=4.37 kbar; $\bar{U}_{se}$=5.027 mm/μsec									
30% Ni–70% Fe bcc									
0.2735	12.79	0.1368	...	5.14	...	...	49.8	0.9708	0.1347
0.1126	12.79	0.0563	...	...	...	...	21.8	0.9876	0.0578
0.0922	12.79	0.0461	...	5.11	...	...	17.9	0.9900	0.0471
Mean density 8.032 g/cm³; C_0=5.23 mm/μsec; $\bar{U}_{se}$=5.13 mm/μsec									
36% Ni–64% Fe fcc									
0.2853	12.72	0.1427	...	4.91	4.3	0.9977	44.2	0.9646	0.1452
0.1878	12.74	0.0939	...	4.84	5.3	0.9972	30.8	0.9752	0.0968
0.1090	12.74	0.0545	...	...	5.3	0.9972	18.2	0.9865	0.0550
Mean density 8.077 g/cm³; C_0=4.73 mm/μsec; σ_e=5.0 kbar; $\bar{U}_{se}$=4.88 mm/μsec									

[a] Measured impact velocity.
[b] Particle velocity imparted to the specimen for symmetrical impacts.
[c] Stress imparted to the specimen as measured by a quartz gage.
[d] Wave velocity of elastic wave.
[f] Hugoniot elastic limit.
[g] Relative volume at Hugoniot elastic limit.
[h] Maximum stress of plastic wave.
[i] Computed relative volume of plastic wave.
[j] Maximum particle velocity of second plastic wave.
[k] Final stress value was not recorded due to partial experimental failure. The value shown was adjusted to agree with the input value.
[l] Impact surface experiment only. The initial temperature of the sample was 130°C.
[m] Low signal dilatational velocity as obtained by ultrasonic pulsing.
[n] Low signal shear-wave velocity as obtained by ultrasonic pulsing.

used. The velocity of the impacting surface is measured to ±0.5%; therefore, if like materials are used for the projectile and sample, the particle velocity imparted to the sample is known. Also, impacting with a quartz gage enables a measurement of the stress and particle velocity imparted to the sample at the impact face.[14,15] These data provide independent measurements of the shock-wave behavior from that obtained at the conventional measuring station at the back side of the specimen. The redundancy achieved allows cross comparisons of data from a single experiment and greatly increases the confidence in the results since it serves as a quantitative measure of errors in the entire data recording and data reduction process as well as a verification of the assumptions made in reducing the data.

Shock-wave velocity data are needed to compute the stress amplitude in the sample from the observed quartz gauge record of the interface stress. These measurements are accomplished by the arrival times indicated by the impacting and back surface quartz gauges with accurately known time delays interposed between trigger signals for two-gauge records. For the experiments in which an impacting gauge is not used, the discharge of charged coaxial pins is used to indicate impact time. The shock-wave velocity accuracy is ±1%. The absolute error in stress is ±3% with ±1% relative errors. The error in volume change is estimated to be ±2%.

The 30% Ni–70% Fe alloy material was the commercially obtained "Temperature Compensator 30" alloy.[16] The 36% Ni–Fe alloy used was "Invar 36" obtained from the same supplier. After machining to the desired dimensions, the samples were heat treated according to the following schedule. The fcc phase 30% Ni alloy samples were held 2 h at 650°C, then furnace-cooled to 100°C. The bcc phase 30% Ni alloy samples were annealed 2 h at 650°C, furnace cooled to room temperature, then kept in liquid nitrogen for 168 h. The 36% Ni–Fe alloy samples were held 16 h at 900°C, then furnace cooled to 100°C. All elevated temperature treatments were performed in a vacuum of 10^{-6} Torr.

[14] W. J. Halpin, O. E. Jones, and R. A. Graham, ASTM Special Technical Publication No. 336, ASTM (1962).
[15] W. J. Halpin and R. A. Graham, Fourth Symposium on Detonation, U.S. Naval Ordnance Laboratory (October 1965).
[16] The alloys were obtained from the Carpenter Steel Company.

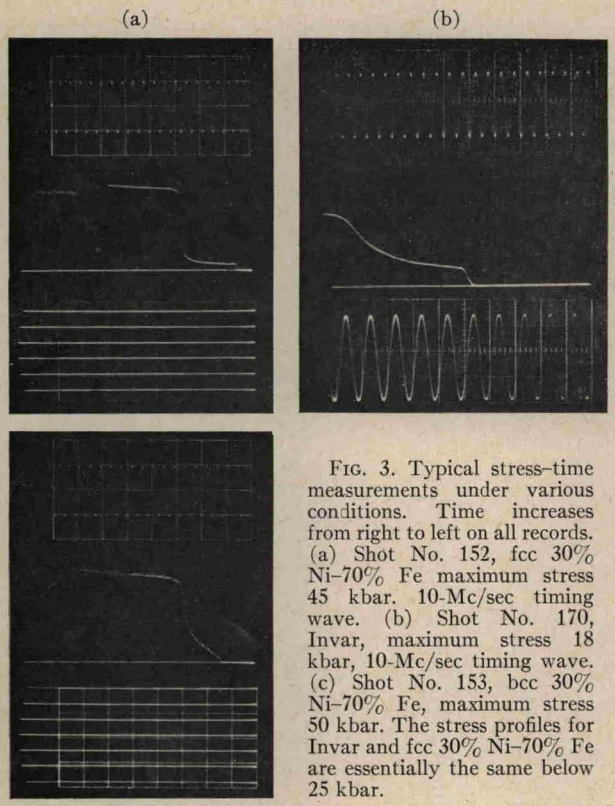

FIG. 3. Typical stress–time measurements under various conditions. Time increases from right to left on all records. (a) Shot No. 152, fcc 30% Ni–70% Fe maximum stress 45 kbar. 10-Mc/sec timing wave. (b) Shot No. 170, Invar, maximum stress 18 kbar, 10-Mc/sec timing wave. (c) Shot No. 153, bcc 30% Ni–70% Fe, maximum stress 50 kbar. The stress profiles for Invar and fcc 30% Ni–70% Fe are essentially the same below 25 kbar.

X-ray examination of the heat-treated samples showed that to the limit of detectability (5%) no minority phase was present. To determine atmospheric pressure elastic constants, typical samples were pulsed ultrasonically with results as shown in Table I. Chemical analyses were obtained on the samples which, for a given alloy, were all cut from the same bar of material. The mean value for the nickel content was 29.53% with a variance of 0.24%.

Since it was desired to measure the change in Curie temperature with pressure, it was necessary to measure the atmospheric-pressure Curie temperature for the 30% Ni–Fe alloy. This was determined by dilatometer measurements on bulk samples and x-ray lattice spacing vs temperature measurements. The value obtained for the Curie temperature from the thermal expansion measurements was 155°±3°C.

RESULTS

Typical stress–time profiles for various materials and various stress regions are shown in Fig. 3. The leading part of the profile results from the transition from elastic to plastic deformation. The sharp rise in stress for the second wave in Fig. 3(a) and the faster arrival time compared with that in Fig. 3(b) is that expected if the input stress is above the transition. Whereas, the slower rise in Fig. 3(b) is that expected if the stress input to the sample is below the transition. The profile in Fig. 3(c) for the bcc alloy was obtained for an imput particle velocity approximately equal to that in Fig. 3(a) for the fcc alloy. The bcc alloy shows a poorly defined precursor region, but, in any event, much faster arrival times are observed for all stress amplitudes as is indicative of lower compressibility.

The excellent time-resolution of the quartz gauge has revealed that few materials give idealized step function stress–time profiles. Hence, to reduce the stress–time profiles to stress–volume points the profile observed must be approximated by a series of small incremental steps constructed around the observed profile. This procedure has the further advantage that corrections can be made for the slightly variable response of the gauge. The solution for the incident stress from the measured interface stress was accomplished for each small increment of stress using the linear mismatch relations and the appropriate shock velocity for each step. The resulting final values can be checked against the measured input conditions to the sample as an over-all check of experimental errors and errors in data reduction. The data obtained on all experiments are tabulated in Table I. Most of the experiments were performed on fcc 30% Ni with less extensive experiments on 36% Ni and bcc 30% Ni.

The resulting stress–volume relations for the 30% Ni alloys are shown in Fig. 4. The cusp in the fcc curve at 4.3 kbar is the mean value observed for the Hugoniot

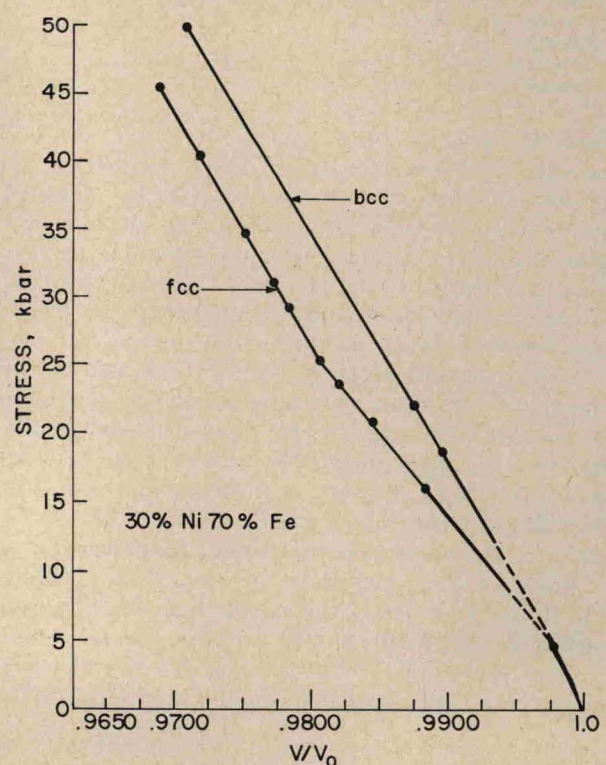

FIG. 4. Stress–volume relation for 30% Ni–70% Fe in the fcc and bcc phases.

elastic limit, whereas the dashed line shown for the fcc alloy indicates the stress region for which some strain hardening is indicated from the stress profiles. It is readily apparent that below 25 kbar the fcc alloy shows a much larger compressibility than the bcc alloy.

ANALYSIS

The compressibility of the fcc alloy shows a large, well-defined change at 25 kbar, clearly indicating the expected behavior for a second-order phase transition. The anomalously high value of the compressibility for the pressure-sensitive fcc alloy is demonstrated in the comparison of compressibilities of various ferromagnetic iron alloys in Table II.[17–19] The fcc 30% Ni alloy as well as the Invar alloy have compressibilities which are far in excess of the normal values for the ferromagnetic iron alloys whose magnetic properties are not pressure sensitive. Further, for stress in excess of the stress required to induce the transition to the nonmagnetic state, the compressibilities of both 30% Ni and Invar have a normal value. Invar does not show a well-defined transition, but its roughly analogous behavior to that of the fcc 30% Ni alloy shows that magnetic effects are responsible for the pressure induced change in compressibility.

TABLE II. Compressibilities of various iron alloys.

Material	$-(1/V)(\Delta V/\Delta P)$, 10^{-4} kbar^{-1} Shock wave compression	Low signal adiabatic
Pressure-sensitive ferromagnetic iron alloys		
30% Ni 70% Fe, fcc	8.6[a]	8.97[a]
36% Ni 64% Fe, fcc	8.8[a]	8.9[b]
Pressure-insensitive ferromagnetic iron alloys		
30% Ni 70% Fe, bcc	6.0[a]	6.6[c]
Armco Fe, bcc	6.4[d]	5.93[e]
30% Ni 70% Fe, fcc. Stress range above transition stress	5.8[a]	...
36% Ni 64% Fe, fcc. Stress range above transition	5.0[f]	...
30% Ni 70% Fe, fcc. Elevated temperature (130°C)	6.4[g]	...

[a] As determined in the present investigation.
[b] Computed from Young's modulus and Poisson's ratio as given in Ref. 6.
[c] As given by Ref. 17.
[d] Data from Ref. 18. Stress range from 40 to 55 kbar.
[e] Reference 19.
[f] Data from Ref. 12. Stress range from 70 to 110 kbar.
[g] As determined in the present investigation. The computation assumes that the Hugoniot elastic limit does not change with temperature; thus, this value is somewhat more uncertain than the other values.

[17] E. P. Papadakis and E. L. Reed, J. Appl. Phys. **32**, 682 (1961).
[18] D. S. Hughes, L. E. Gourley, and M. F. Gourley, J. Appl. Phys. **32**, 624 (1961).
[19] D. S. Hughes and C. Maurette, J. Appl. Phys. **27**, 1184 (1956).

To further clarify the role of magnetic effects on compressibility, a shock compression experiment was performed on an fcc 30% Ni sample whose initial temperature was raised to 130°C. As is shown in Table II, the compressibility was found to decrease to a value consistent with the nonmagnetic compressibility. Thus, the sharp change in compressibility, the critical values for the transition, and the magnitudes of the compressibility under the various conditions give a clear demonstration that a second-order magnetic transition has been observed and we will proceed with a quantitative analysis of the transition.

PROPERTIES OF THE TRANSITION

The experiments result in an explicit measure of the change in the shock-wave compressibility which occurs at 25 kbar. For the small compressions involved (2% at 25 kbar), the shock-wave compression is adiabatic to a very close approximation. Thus, the isothermal compressibility Δk_T can be computed from the thermodynamic relation between adiabatic and isothermal compressibilities.[20] Further, from the pressure and temperature of the transition, the coefficient $d\theta/dP$ can be computed. The evaluation of both Δk_T and $d\theta/dP$ allow the change in thermal expansion and specific heat to be computed from Eqs. (1) and (2), and a complete description of the properties of the transition is then obtained.

The temperature at the transition is the initial temperature[21] of the sample plus the shock-wave heating which occurs. This temperature rise is only 3°C up to the transition,[22] and is small enough that uncertainties in the change in Curie temperature are principally due to the measurement of Curie temperature at atmospheric pressure. Thus, the Curie temperature is lowered from 155°C to 25°C due to the stress of 25 kbar.

The small but significant component of shear stress that is associated with the elastic compression results in a stress configuration which is not hydrostatic. Thus, the shock-wave experiment measures a longitudinal component of stress rather than the pressure of the transition. Belov has shown that shear stress does not change the Curie temperature or saturation magnetiza-

[20] $\Delta k_T = \Delta k_s[1+T(\beta_1\gamma_1-\beta_2\gamma_2)]$, where Δk_s is the change in adiabatic compressibility at the transition and γ is the Grüneisen ratio. The subscripts 1 and 2 refer to values in the low-pressure and high-pressure phases, respectively. β_1 is taken as zero in agreement with data to be shown later, β_2 is taken as 4.4×10^{-5} °C^{-1} and C_P is taken as 1.2×10^{-1} cal g^{-1} °C^{-1}.
[21] The experiment is conducted in a temperature-controlled room at 22°C.
[22] The temperature is computed as $T_s = T_0(V_0/V)^\gamma$ where γ is the appropriate Grüneisen's ratio which is computed from the relation $\gamma = \beta C_P/k_s V$. As is shown later, our best estimate is that γ decreases from its room-temperature value, 0.85, to zero at a stress just below the transition due to the decrease in thermal expansion. Since the volume change and temperature rise are small, we choose γ as 0.43, a mean value over the pressure range. This is admittedly crude, but the difference between this calculation and a more sophisticated analysis is insignificant.

TABLE III. Values for the coefficient of Curie temperature change with pressure, $d\theta/dP$.

Patrick[a]	-5.7 ± 0.2°C kbar^{-1}
Belov[b]	-5.4
Kaneko[c]	-3.2
Samara[d]	-5.5
Present work	-5.8 ± 0.3

[a] Curie temperature shift determined by susceptibility measurements. Maximum pressure 5 kbar. Ref. 2.
[b] Calculated from volume magnetostriction measurements at atmospheric pressure, Ref. 23.
[c] Curie temperature shift determined by magnetization-temperature measurements. Maximum pressure 3 kbar. Ref. 25.
[d] Curie temperature shift determined by susceptibility measurements. Maximum pressure 25 kbar. Ref. 26.

tion of these alloys.[23,24] His values for $d\theta/dV$ measured in uniaxial stress (which results in a large shear stress) are the same as those obtained hydrostatically. Thus, it is the volume, $0.9807V_0$, which is characteristic of the transition. To compare our values to the previous hydrostatic pressure values, an equivalent pressure must be computed from our observed value for the volume at the transition. The equivalent pressure is computed from our measured compressibility and the volume change to induce the transition. This yields a value of 22.6 kbar for the equivalent pressure of the transition. From this value of the equivalent pressure and the temperature change induced by this pressure, the value of $d\theta/dP$ is calculated to be -5.8°C kbar^{-1}. Our value is an average value over the entire pressure range. As shown in Table III,[25,26] this value is in good agreement with most of the previous investigators; therefore, we conclude that $d\theta/dP$ is constant over the entire pressure range encountered.

The thermodynamic description of the transition can now be completed since we now have a measure of both Δk_T and $d\theta/dP$ and can calculate $\Delta\beta$ and ΔC_p from Eqs. (1) and (2) with results as summarized in Table IV. Thus, these experiments provide a complete description of the thermodynamic properties of the transition.

DISCUSSION

The value of the change in thermal expansion coefficient accompanying the transition is considerably larger than that obtained when the transition is thermally induced at atmospheric pressure. That is, our value for the thermal expansion at 22°C and atmospheric pressure is 3.0×10^{-5} °C^{-1} and for temperatures above the transition temperature the value is 5.1×10^{-5} °C^{-1} which is a normal paramagnetic value for alloys in this composition range. Since the change in thermal expansion which occurs at the pressure induced transition is $+4.7\times10^{-5}$ °C^{-1}, a normal value for the thermal expansion in the high-pressure paramagnetic state implies that in the low-pressure ferromagnetic state the thermal expansion coefficient decreases strongly with pressure to a value close to zero immediately before the transition.

Although there are no direct measurements of the thermal expansion coefficient of this alloy at various pressures, compressibility vs temperature measurements have been made.[27] From these compressibility data and thermodynamic identity $\partial\beta/\partial P=-\partial k/\partial T$ the initial slope of the thermal-expansion–pressure relation can be computed at atmospheric pressure. This initial slope is found to be $+1.7\times10^{-6}$ °C^{-1} kbar^{-1} which is in contradiction to the behavior we have inferred from our high-pressure measurements. However, the extrapolation of initial slopes at atmospheric pressure to high pressures where there are large changes in the magnetic interactions is clearly an uncertain procedure. Thus, the most likely behavior of the thermal expansion coefficient with pressure is an initial small increase followed by a continual decrease in slope until a large negative slope is obtained.

The thermal expansion data appear to be applicable to an interpretation of the physical nature of the magnetic interactions and their change with pressure. Kouvel and Wilson,[3] and Kondorsky and Sedov[28] have postulated that the unusual volumetric behavior of the magnetic interactions is a result of a mixed ferromagnetic, antiferromagnetic coupling. The iron–iron interactions are thought to be antiferromagnetic whereas the Ni–Ni and Ni–Fe interactions are ferromagnetic. Weiss[29] has discussed the possibility that fcc iron has two electronic states and has calculated the thermal-expansion–temperature relation predicted on this basis. It may be possible to examine such physical models on the basis of

TABLE IV. Characteristics of the pressure-induced magnetic transition in fcc 30% Ni–70% Fe.

Specific volume	$0.9807\ V_0$
Temperature (°C)	25
Equivalent pressure (kbar)	22.6
$d\theta/dP$ (°C kbar^{-1})	-5.8 ± 0.3
Δk_T (kbar^{-1})	$-2.72\pm0.05\times10^{-4}$
ΔC_p (cal g^{-1} °C^{-1})	$-7.2\pm0.7\times10^{-3}$
$\Delta\beta$ (°C^{-1})	$+4.7\pm0.5\times10^{-5}$

[23] K. P. Belov, *Magnetic Transitions* (Consultants Bureau, New York, 1961), p. 98.
[24] K. P. Belov and A. M. Kadomtseva, *On the Influence of Unilateral Elastic Deformations on the Curie Point of Ferromagnetics*, Sandia Corporation Translation, SC-T-64-1648 (November 1964), Translation of Vestnik Mosk. Univ. No. 2, 133 (1958).
[25] T. Kaneko, J. Phys. Soc. Japan **15**, 2247 (1960).
[26] G. A. Samara, Sandia Laboratory (private communication).
[27] G. A. Alers, J. R. Neighbors, and H. Sato, J. Phys. Chem. Solids **13**, 40 (1960).
[28] E. T. Kondorsky and V. L. Sedov, J. Appl. Phys. Suppl. **31**, 331 (1960).
[29] R. J. Weiss, Proc. Phys. Soc. (London) **82**, 281 (1963).

a theoretical thermal-expansion–pressure relation, but this is beyond the scope of the present work.

The discontinuous changes in compressibility and thermal expansion which occur when the transition is induced with pressure are in sharp contrast to the more or less continuous changes in thermal expansion and compressibility which occur in the thermally induced transition.[27] The difference is believed to arise because the effects of pressure proceed at essentially constant temperature, whereas, the effects of temperature do not occur at constant volume. For this alloy, the exchange interactions are extremely volume dependent and the volume change resulting from the thermal expansion is sufficient to alter the magnetic exchange interactions by a significant amount. Consequently, to consider thermally induced disorder alone, the thermal expansion and compressibility should be analyzed at constant volume. It appears that most measurements of the effect of temperature on the magnetic and physical properties of this alloy have considered the Curie temperature fixed even though the temperature changes have been sufficient to produce large volume changes which would alter the exchange interactions.

In summary, this paper has reported shock-wave measurements of the compressibility of fcc 30% Ni–70% Fe which show a well-defined, pressure-induced, second-order ferromagnetic to paramagnetic transition. From these measurements, a complete description is obtained of the thermodynamic variables which change at the transition. The results provide a more complete description of the thermodynamic effects of the change in the magnetic interactions with pressure than has been previously available.

ACKNOWLEDGMENTS

The authors are pleased to acknowledge the technical assistance of W. D. Ingram, the sound velocity measurements by Dr. Barry Butcher, the specimen design and instrumentation by G. E. Ingram, and many useful discussions with their Sandia Laboratory colleagues. The reviewer was quite helpful in interpretation of some of the previous results.

Issued by
Technical Information Division III
Sandia Corporation
Albuquerque, New Mexico